

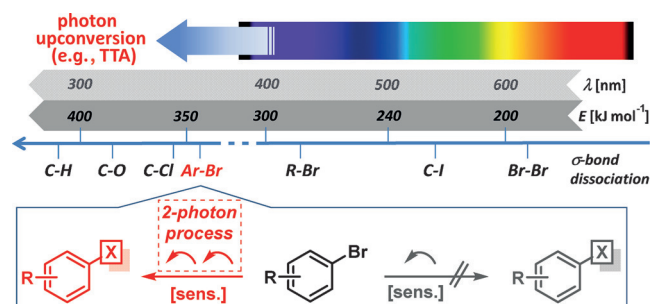
## Photocatalysis | Very Important Paper |

## VIP Application of Visible-to-UV Photon Upconversion to Photoredox Catalysis: The Activation of Aryl Bromides

Michal Majek,<sup>[a]</sup> Uwe Faltermeier,<sup>[b]</sup> Bernhard Dick,<sup>[b]</sup> Raúl Pérez-Ruiz,<sup>\*,[a]</sup> and Axel Jacobi von Wangelin<sup>\*,[a]</sup>

**Abstract:** The activation of aryl–Br bonds was achieved by sequential combination of a triplet–triplet annihilation process of the organic dyes, butane-2,3-dione and 2,5-diphenyloxazole, with a single-electron-transfer activation of aryl bromides. The photophysical and chemical steps were studied by time-resolved transient fluorescence and absorption spectroscopy with a pulsed laser, quenching experiments, and DFT calculations.

The recent developments of chemical reactions mediated by visible light as an abundant source of energy have significantly expanded the toolbox of modern organic synthesis.<sup>[1]</sup> The scope of photocatalytic bond activations is generally limited by the energy of the visible photon, which in principle allows the cleavage of weak C–I, C(sp<sup>3</sup>)–Br and  $\pi$  bonds by energy or electron-transfer mechanisms.<sup>[2]</sup> However, a single visible photon does not provide sufficient energy for the dissociation of the stronger aryl–Br, C–Cl, C–O, and C–H bonds.<sup>[3]</sup> Accordingly, visible-light-mediated aromatic functionalization protocols require the use of highly electrophilic arenediazonium salts or aryl iodides.<sup>[4]</sup> The bond-dissociation energy (BDE) of aryl–Br bonds (Ph–Br: 346 kJ mol<sup>-1</sup>) considerably exceeds the maximum photonic energy of visible light (300 kJ mol<sup>-1</sup>). The reduction potentials of non-activated aryl bromides (PhBr: –2.68 eV vs. SCE)<sup>[5]</sup> are also beyond the excited triplet energies of common photoactive one-electron reductants (eosin Y: 1.9 eV; [Ru(bpy)<sub>3</sub>]<sup>2+</sup>: 2.0 eV; [Ir(ppy)<sub>3</sub>]<sup>+</sup>: 2.5 eV),<sup>[6]</sup> even more so when considering the energy loss during intersystem crossing (ISC) and structural reorganizations. This limitation could be overcome by the implementation of two-photon processes, such as photon upconversion (UC).<sup>[7]</sup> Among the different UC mechanisms, the sensitized triplet–triplet annihilation (TTA) operates at especially low incident light power.<sup>[8]</sup> This type of UC process involves an energy transfer between a sensitizer



Scheme 1. Application of a two-photon process to the activation of aryl–Br.

(donor) and annihilator (acceptor) and ultimately leads to anti-Stokes shifted fluorescence (Scheme 1). TTA allows the additive combination of the energies of two long-lived excited triplet states of the annihilator to reach its excited singlet state.<sup>[9]</sup> TTA properties of a few combinations of sensitizers and annihilators were studied over the past years. Despite the fact that the use of low-energy visible light ensures high functional-group tolerance in chemical transformations, applications of TTA have been limited to the direct observation of delayed fluorescence or energy-transfer processes, the latter mostly involving the generation of singlet oxygen. There are no applications to critical bond activations or electron transfers in organic synthesis. Stimulated by the rapid progress in photocatalytic aromatic substitutions,<sup>[2–4]</sup> we probed the feasibility of combining a TTA process with a chemical redox reaction of hitherto unreactive aryl bromides (Scheme 1).

We initially chose the simple metal-free couple butane-2,3-dione (**BD**, sensitizer) and 2,5-diphenyloxazole (**PPO**, annihilator), which was reported to exhibit low power Vis-to-UV photon upconversion, but has not been applied to a chemical reaction.<sup>[10]</sup> This system allowed selective excitation of **BD** (at 430 nm) in the presence of **PPO** by laser flash photolysis (LFP) in a  $\mu$ s time domain.<sup>[11]</sup> The resultant formation of <sup>1</sup>PPO\* was also observed under different conditions in degassed DMF by its characteristic delayed fluorescence at 370 nm, which corresponds to an excited singlet-state energy of 3.35 eV (Figure 1). The fluorescence of **BD** was observed between  $\lambda = 450$ –500 nm together with the incident laser pulse (Figure 2).<sup>[10,11]</sup>

Under these conditions, the lifetime of <sup>1</sup>PPO\* (1.3  $\mu$ s) was determined from a mono-exponential fit of the decay trace at 370 nm (Figure 2, inset). In the triplet–triplet annihilation (TTA) event, the population of <sup>1</sup>PPO\* is achieved by the collision of two molecules in the triplet excited state (<sup>3</sup>PPO\* + <sup>3</sup>PPO\*). As-

[a] M. Majek, Dr. R. Pérez-Ruiz, Prof. Dr. A. Jacobi von Wangelin  
Institute of Organic Chemistry, University of Regensburg  
Universitaetsstrasse 31, 93040 Regensburg (Germany)  
E-mail: raul.perez-ruiz@ur.de  
axel.jacobi@ur.de

[b] U. Faltermeier, Prof. Dr. B. Dick  
Institute of Physical and Theoretical Chemistry  
University of Regensburg  
Universitaetsstrasse 31, 93040 Regensburg (Germany)

Supporting information for this article is available on the WWW under <http://dx.doi.org/10.1002/chem.201502698>.

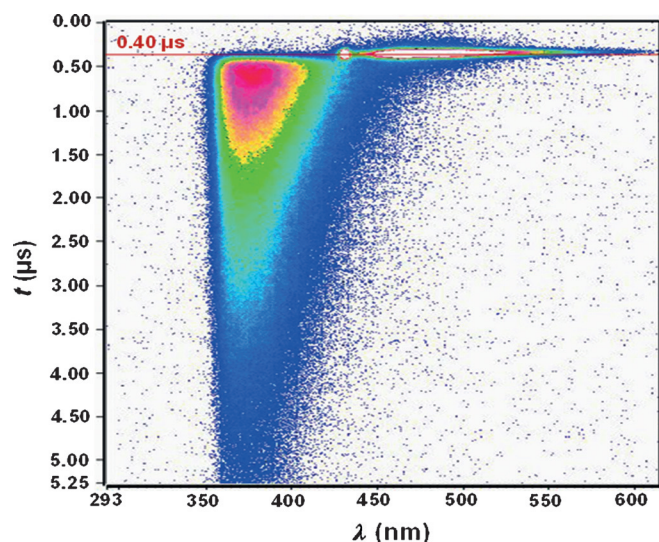


**Figure 1.** 2D Transient fluorescence matrix of a mixture of **BD** (0.04 M) and **PPO** (0.013 M) in degassed DMF from pulsed laser excitation at 430 nm at 0.4  $\mu$ s after start of recording).

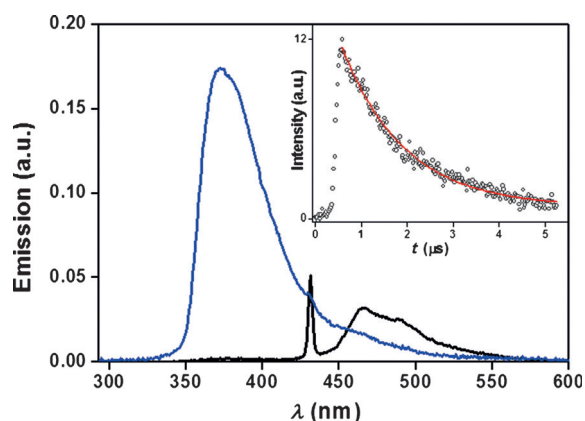


**Figure 2.** Sum of emission spectra from 0–0.4  $\mu$ s (black line) and 0.4–3  $\mu$ s (blue line). Inset: decay trace monitored at 370 nm and mono-exponential fit (red line).

suming that  $^1\text{PPO}^*$  is a delayed P-type fluorescence and the overall process is bi-photonic,<sup>[12]</sup> the  $^1\text{PPO}^*$  lifetime is approximately half the value of its precursor  $^3\text{PPO}^*$ . Therefore, LFP experiments ( $\lambda_{\text{exc}}$  430 nm, in DMF under  $\text{N}_2$ ) were performed with **BD/PPO**. Transient absorption spectra displayed the intense band of the triplet absorption of **PPO** at 500 nm.<sup>[10]</sup> A lifetime of 2.3  $\mu$ s was determined from a mono-exponential fit of the kinetic decay of  $^3\text{PPO}^*$  (see the Supporting Information).

Having established the photophysical generation of  $^1\text{PPO}^*$  by a TTA process from visible light, we now set out to study its application to a chemical reaction. As a model system, reductions of three aryl bromides [4'-bromoacetophenone (**1**), 4'-bromobenzotrifluoride (**2**), and 4'-bromoanisole (**3**)] in DMF solution were performed by steady-state photolysis of the **BD/PPO** system. Irradiation of a mixture of **1**, **BD**, and **PPO** with a blue LED light (450 nm, 3.8 W) showed no conversion of **1** after 30 minutes by quantitative GC analysis (Table 1, entry 1), which is due to the low light source power and the

**Table 1.** Light-induced reduction of aryl bromides **1–3** under TTA conditions.<sup>[a]</sup>

Entry	Substrate	Solvent	$t$ [min]	Selectivity [%] <sup>[b]</sup>
1 <sup>[c]</sup>	<b>1</b>	DMF	30	0 (0)
2	<b>1</b>	DMF	10	48 (13)
3	<b>1</b>	DMF	30	88 (19)
4 <sup>[d]</sup>	<b>1</b>	DMF	60	70 (26)
5	<b>1</b>	acetonitrile	30	41 (7)
6	<b>2</b>	DMF	30	71 (6)
7	<b>3</b>	DMF	30	0 (0)

[a] Conditions: 10 mm [Substrate], 40 mm [BD], 13 mm [PPO], under  $\text{N}_2$ ; irradiation with a pulsed laser ( $10 \text{ s}^{-1}$ , 15 mJ) at 430 nm; [b] conversion [%] in parentheses; calculated from quantitative GC-FID versus internal *n*-pentadecane; [c] irradiation with blue LED (450 nm, 3.8 W); [d] after 30 min irradiation addition of another 40 mm **BD** and irradiation for 30 min.

mismatch of irradiation and absorption maxima (450 vs. 430 nm). Then, steady-state irradiations were carried out by using a pulsed laser ( $10 \text{ s}^{-1}$ , 15 mJ pulse<sup>-1</sup>). Indeed, low conversion of **1** and high selectivity was observed (Table 1, entry 3). Further addition of **BD** and irradiation gave higher conversions, which can be a consequence of slow decomposition of **BD**, most likely by H-atom transfer from the solvent DMF to  $^3\text{BD}^*$  (entry 4).<sup>[13]</sup> The presence of a less activating substituent in **2** led to low (entry 6), a deactivating substituent in **3** to no conversion (entry 7), presumably due to the more negative reduction potentials. The involvement of  $^1\text{PPO}^*$  as high-energy intermediate was proven by quenching experiments. Upon addition of increasing amounts of **1** or **2**, respectively (Figure 3 and the Supporting Information), a significant decrease of  $^1\text{PPO}^*$  fluorescence was observed, whereas no quenching was effected with the unreactive **3** (see the Supporting Information).

Interestingly, the  $^1\text{BD}^*$  intensity was not affected by the presence of **1**, which rules out a direct electron transfer from  $^1\text{BD}^*$ . The quenching rate constants were derived from Stern–Volmer analyses [Eq. (1), Eq. (2), and Figure 2 inset]:

$$\frac{I_0}{I} = 1 + K_{\text{sv}}[\text{C}] \quad (1)$$

$$K_{\text{sv}} = \tau_s k_q(S_1) \quad (2)$$

The Stern–Volmer constants ( $K_{\text{sv}}$ ) and rate constants of singlet quenching  $k_q(S_1)$  based on the fluorescence lifetime of **PPO** ( $\tau_s = 1.4 \text{ ns}$ , see the Supporting Information)<sup>[13]</sup> are given in Table 2. These data suggest nearly diffusion-controlled quenching of  $^1\text{PPO}^*$  by **1**. For the less activated aryl bromide **2** and deactivated aryl bromide **3**, the quenching rate constants  $k_q(S_1)$  are one and two orders of magnitude lower, respectively, which indicates a low kinetic contribution of this electron transfer (ET) process. The relative contributions of the different

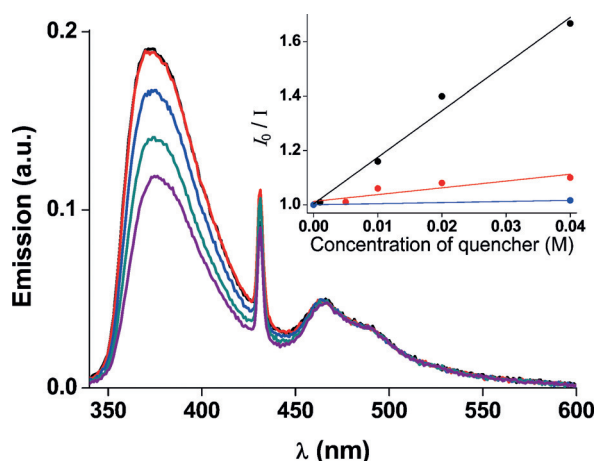


**Figure 3.** Emission spectra of a mixture of **BD** (0.04 M) and **PPO** (0.013 M) in degassed DMF after excitation with a pulsed laser (430 nm at 0.4  $\mu$ s) recorded from 0 to 5  $\mu$ s in the presence of increasing amounts of **1**. Inset: Stern–Volmer plots of **1** (black dot), **2** (red dot), and **3** (blue dot) for the determination of  $k_q(S_1)$ .

S <sup>[a]</sup>	$K_{SV}$ <sup>[b]</sup>	$10^{10}k_q$ <sup>[c]</sup>	Q/F/ISC <sup>[d]</sup>	$E_{red}$ <sup>[e]</sup>	$\Delta G_{ET}(S_1)$ <sup>[f]</sup>	$\Delta G_{ET}(T_1)$ <sup>[f]</sup>
1	18.0	1.3	33/56/11	−1.83	−7	+22
2	2.5	0.18	7/79/14	−2.42	+6	+36
3	0.4	0.03	1/84/15	−2.84	+16	+46

[a] Substrate (= quencher); [b] Stern–Volmer constant in  $\text{M}^{-1}$ ; [c]  $^1\text{PPO}^*$  quenching rate constant  $k_q$  in  $\text{M}^{-1}\text{s}^{-1}$ ; [d] relative contribution of quenching (Q), fluorescence (F), intersystem crossing (ISC) pathways to  $^1\text{PPO}^*$  deactivation in %; [e] reduction potential of quenchers 1–3 versus SCE in eV; [f] free energy of SET from  $^1\text{PPO}^*$  ( $S_1$ ) or  $^3\text{PPO}^*$  ( $T_1$ ) calculated from Equation (5) in  $\text{kcal mol}^{-1}$ .

deactivation pathways of  $^1\text{PPO}^*$  were calculated from Equation (3). The rate constants of fluorescence ( $k_f$ ) and intersystem crossing ( $k_{isc}$ ) are intrinsic properties of the photosensitizer. The  $k_f$  value for **PPO** was calculated from Equation (4); the fluorescence quantum yield ( $\Phi_f$ ) was experimentally obtained ( $\Phi_f = 0.31$  in DMF; see the Supporting Information for calculations). Value of  $k_f$  was determined to be  $2.2 \times 10^8 \text{ s}^{-1}$  (with  $k_{isc} = 4 \times 10^7 \text{ s}^{-1}$ ).<sup>[14]</sup>

$$k_D(S_1) = k_q(S_1)[S] + k_f + k_{isc} \quad (3)$$

$$\tau_s k_f = \Phi_f \quad (4)$$

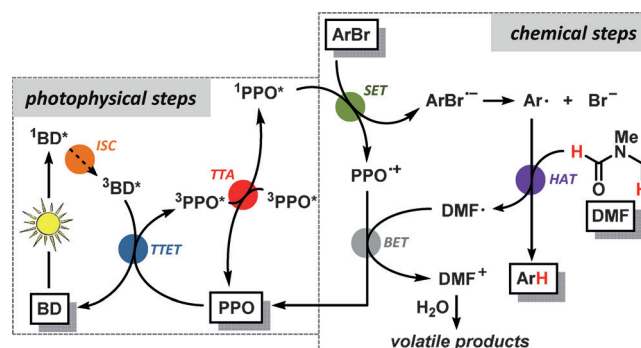
Under the irradiation conditions ( $[S] = 10^{-2} \text{ M}$ ), the direct quenching of  $^1\text{PPO}^*$  by **1** contributes considerably to the overall singlet deactivation, whereas this pathway proceeds weakly for **2** and is nearly irrelevant for **3**. There is a good correlation between these results and the experimental results from the preparative steady-state photolysis shown in Table 1. However, there is still a significant portion of excited molecules of **PPO** (ca. 11%), which undergo ISC to the excited triplet state in the case of **1**. Spectroscopic transient absorption measurements

were performed to ascertain whether the SET occurs from the  $^3\text{PPO}^*$  state. Therefore, increasing amounts of the aryl bromides **1–3** were added to the TTA system (40 mM **BD**, 13 mM **PPO** in DMF,  $\text{N}_2$ , irradiation at  $\lambda = 430 \text{ nm}$ ) to determine the triplet quenching rate constants. In all cases, absorption at  $\lambda = 500 \text{ nm}$  was unaffected by the presence of the aryl bromides (see the Supporting Information). Furthermore, the decay kinetics data of  $^3\text{PPO}^*$  were coinciding even at high quencher concentrations, which is indicative of a lack of triplet quenching.

The free energies of the electron transfer from both the  $S_1$  and  $T_1$  states of **PPO** were obtained from the Weller Equation [Eq. (5), Table 2].<sup>[15]</sup> The reduction potentials of **1–3** (Table 2) and the oxidation potential of **PPO** (1.46 V vs. SCE) were obtained by cyclic voltammetry (CV) under identical conditions in DMF. The energy of the  $S_1$  state of **PPO** was determined from the intersection of the normalized emission and excitation bands of **PPO** ( $10^{-4} \text{ M}$ ) in DMF ( $83 \text{ kcal mol}^{-1}$ ); the  $T_1$  energy ( $53 \text{ kcal mol}^{-1}$ ) was previously reported.<sup>[10]</sup> Consequently, the SET from  $^1\text{PPO}^*$  appeared to be exergonic for **1**, whereas an ET mechanism from  $^3\text{PPO}^*$  is thermodynamically unfeasible for all aryl bromides.

$$\Delta G_{ET} = 23.06[E_{ox} - E_{red}] - E^*(S_1 \text{ or } T_1) \quad (5)$$

We postulate the operation of a new mechanism for the reductive activation of aryl bromides by sequential TTA, single-electron transfer (SET), and H atom abstraction (HAT), which is in agreement with the collected experimental results (Scheme 2). Selective excitation of **BD** at 430 nm and efficient ISC ( $\Phi_{isc} \approx 1$ )<sup>[10]</sup> generate the  $^3\text{BD}^*$  state, which relaxes to **BD** upon triplet–triplet energy transfer (TTET) with **PPO**. At sufficiently high concentrations of the resultant long-lived  $^3\text{PPO}^*$ , a collision between two  $^3\text{PPO}^*$  molecules populates the  $^1\text{PPO}^*$  state, which shows the characteristic anti-Stokes fluorescence maximum of the TTA process at 370 nm. The same species induces SET to the electrophilic aryl bromide, possibly being the rate-limiting step (see below) and affords the unstable radical anion  $\text{ArBr}^{\cdot-}$ , which fragments to the aryl radical  $\text{Ar}^\cdot$ . Rapid H-atom abstraction from the solvent DMF gives the formal reduc-



**Scheme 2.** Postulated mechanism involving TTA, SET, and HAT as key steps. ISC = intersystem crossing; TTET = triplet–triplet energy transfer; TTA = triplet–triplet annihilation; SET = single-electron transfer; HAT = H-atom transfer; BET = back-electron transfer.

tion product Ar–H. The resultant radical DMF<sup>•</sup> regenerates PPO by an exergonic back-electron transfer to give highly electrophilic DMF<sup>+</sup>, which hydrolyzes upon work-up to volatile products.<sup>[16]</sup>

To explain the differences in reactivity between aryl bromides 1–3, we have also investigated kinetic aspects of the reaction mechanism. It is well established that the fragmentation of aryl bromide radical anions (ArBr<sup>•-</sup>) to the respective aryl radicals Ar<sup>•</sup> and Br<sup>-</sup> proceeds rapidly under the experimental conditions.<sup>[9a]</sup> Further, we assume that the low activation energies of HAT from DMF to Ar<sup>•</sup> and the large excess amounts of DMF as solvent make this step very rapid.<sup>[16]</sup> This suggests that the SET from <sup>1</sup>PPO\* to the aryl bromides is most likely the rate-determining step. Therefore, we used the Marcus theory to determine the activation barriers of the SET steps  $\Delta G_{\text{SET}}^{\ddagger}$  which can be obtained from the free energy of the reaction  $\Delta G_{\text{SET}}^0$  and the nuclear reorganization energy  $\lambda$  [Eq. (6) and Table 3].<sup>[17]</sup>

$$\Delta G_{\text{SET}}^{\ddagger} = \frac{(\Delta G_{\text{SET}}^0 + \lambda)^2}{4\lambda} \quad (6)$$

S <sup>[a]</sup>	$\Delta G_{\text{ET}}^{\ddagger}$ (calcd) <sup>[b]</sup>	$\Delta G_{\text{ET}}^{\ddagger}$ <sup>[c]</sup>	$\Delta G_{\text{BET}}^{\ddagger}$ <sup>[d]</sup>	$\Delta G_{\text{GS-BET}}^{\ddagger}$ <sup>[e]</sup>
1	-7	0.1	6.8	119
2	+9	9.5	0.4	104
3	+22	29.9	7.8	272

[a] Substrate (= quencher); [b] free energy of SET from <sup>1</sup>PPO\* (S<sub>1</sub>) to S calculated by DFT in kcal mol<sup>-1</sup>; [c] activation energy of SET from <sup>1</sup>PPO\* (S<sub>1</sub>) to S calculated by DFT in kcal mol<sup>-1</sup>; [d] activation energy of SET from S<sup>-•</sup> to PPO<sup>•+</sup> to form <sup>1</sup>PPO\* (S<sub>1</sub>), calculated by DFT in kcal mol<sup>-1</sup>; [e] activation energy of SET from S<sup>-•</sup> to PPO<sup>•+</sup> to form ground-state PPO (S<sub>0</sub>), calculated by DFT in kcal mol<sup>-1</sup>.

The free energies of the SET process derived from DFT calculations  $\Delta G_{\text{ET}}^{\ddagger}$  (calcd) were in very good agreement with the experimental values obtained from CV measurements (Table 2). The calculated energy barrier for the SET reduction of 1 by <sup>1</sup>PPO\* is negligible, and the energy barrier for the back electron transfer (BET) is 6.8 kcal mol<sup>-1</sup>. This translates to the highest reactivity of 1 with a third of all molecules engaging in a quenching process (Q=33) with <sup>1</sup>PPO\* (Table 2, 4th column, 1st row). The energy barrier for the SET reduction of 2 by <sup>1</sup>PPO\* is still relatively low, but the activation energy for the BET is below 1 kcal mol<sup>-1</sup>, which results in much lower quenching efficiency and low overall reactivity of 2. For *p*-methoxy derivative 3, the SET activation energy is so high that other deactivation mechanism of <sup>1</sup>PPO\* become dominant (Q=1, Table 2). Interestingly, even though the BET from all intermediate S<sup>-•</sup> radical anions to PPO<sup>•+</sup> to give PPO (S<sub>0</sub>) are exergonic, the activation barriers for this process are prohibitively high (Marcus inverted region).

In summary, we have demonstrated a new combination of visible-to-UV photon upconversion and an SET-initiated reductive activation of aryl bromides. The underlying TTA process is

effected by the metal-free dyes BD (sensitizer) and PPO (triplet annihilator). Transient spectroscopy and quenching studies support the formation of <sup>1</sup>PPO\* as high-energy intermediate. The single-electron transfer from <sup>1</sup>PPO\* to the aryl bromides is rate limiting and in combination with the corresponding back-electron transfer determines the overall efficiency of the reaction, as was evidenced by DFT calculations. Further optimization of the photophysical and chemical steps by employing longer lived excited states, lower light power, and more effective quenchers are currently being investigated.<sup>[18]</sup> The general concept of visible-to-UV TTA and other photon-upconversion processes holds great potential for challenging bond activations while retaining the benefit of mild reaction conditions by the use of lower-energy visible light.

## Experimental Section

### Chemicals

Biacetyl (2,3-butanedione), 2,5-diphenyloxazole, 4-bromoacetophenone, 4-bromobenzotrifluoride, 4-bromoanisole, acetophenone, trifluorotoluene, and anisole were commercially available. DMF, extra dry over molecular sieves, acetonitrile (gradient grade), and methanol (for analysis) were used as solvents without further purification.

### General procedure for the steady-state irradiations

A solution of aryl bromide (10 mM) with 2,3-butanedione (40 mM) and 2,5-diphenyloxazole (13 mM) in dry DMF (1 mL) containing *n*-pentadecane (10 mM) as GC internal standard was placed in a 1.5 mL transparent vial with a 8 mm screw cap with butyl/PTFE septum. Then, the solution was irradiated under continuous N<sub>2</sub> purging for 30 min by a pulsed Nd:YAG laser at 430 nm (see the Supporting Information). Then, ethyl acetate (3 mL) was added, and the mixture was washed with brine (5 mL). The organic phase was separated and filtered through MgSO<sub>4</sub> for further analysis. The course of the reaction was followed by quantitative GC-FID analysis on a 7820 A Agilent versus internal *n*-pentadecane. Control experiments showed that photoreduction of aryl bromides 1–3 did not proceed in the dark or in the absence of PPO.

### Gas chromatography (GC)

GC was calibrated by using a four-point calibration versus 10 mM of the internal standard *n*-pentadecane (Std.). GC oven temperature program: initial temperature 50 °C was kept for 0.5 min, the temperature was increased at a rate of 25 °C min<sup>-1</sup> over a period of 9.7 min, until the final temperature (280 °C) was reached and kept for 0.3 min.

### UV/Vis and fluorescence spectroscopy

UV/Vis analyses were performed on a Varian Cary 50 UV/Vis spectrophotometer. Steady-state fluorescence measurements were performed on a Horiba FluoroMax-4 fluorimeter. Excitation and emission slit widths were 1 nm. Hellma quartz SUPRASIL cuvettes (10 × 10 mm; 117.100F-QS) with a screw cap with PTFE-coated silicon septum were used. The PPO concentration was 0.1 mM in both methanol and DMF.

The fluorescence quantum yield in DMF was measured with reference to 2,5-diphenyloxazole ( $\Phi_{\text{F}_0}$  = 0.5 in methanol)<sup>[19]</sup> by compar-

ing the area of fluorescence and absorbance at the excitation wavelength of 330 nm.<sup>[20]</sup>

$$\Phi_F = (a/a_0) \times (A_0 A^{-1}) \times (\eta/\eta_0) \times \varphi_{F0}$$

in which  $\Phi_F$  and  $\Phi_{F0}$ ,  $a$  and  $a_0$ ,  $A$  and  $A_0$  and  $\eta$  and  $\eta_0$  are the quantum yield, area under emission spectra, the absorbance of the sample under study and refractive index of the employed solvent, respectively.

The fluorescence lifetime of PPO was measured by a Ti:Sa Laser System (Libra, Coherent), which provided pulsed laser light. A following optical parametric amplifier (TOPAS-C, Coherent) generates the desired wavelength for excitation with pulse durations of 80 fs. The fluorescence was collected at approximately 30° to the excitation path and detected with a Hamamatsu C7700 streak camera and a Bruker 200is spectrograph.

### Cyclic voltammetry

The redox potentials were measured by cyclic voltammetry with an Autolab PGSTAT302N Metrohm apparatus. All measurements were performed in deaerated DMF containing tetrabutylammonium tetrafluoroborate (0.1 M) as supporting electrolyte, a glassy carbon working electrode, a platinum wire as counterelectrode, a silver wire as pseudo-reference, and ferrocene as internal standard. The scan rate was 0.05 V s<sup>-1</sup>. Potentials are reported with respect to the saturated calomel electrode (SCE).<sup>[21]</sup>

### Laser flash photolysis

The laser flash photolysis system is described in the Supporting Information. All transient spectra were recorded in 3 mL 10 × 10 mm<sup>2</sup> quartz cells. Concentrations of BD and PPO were 40 and 13 mM, respectively, in anhydrous DMF. Concentrations of 1–3 were varied for the quenching experiments from 0, 1, 5, 10, 20 to 40 mM. All experiments were carried out at room temperature under N<sub>2</sub>.

### Computational details

Calculations were performed with the Gaussian 09 software package.<sup>[22]</sup> Geometry optimizations were carried out using the B3LYP functional and 6–31 + G(2d,p) basis set. Geometry of the <sup>1</sup>PPO\* (S<sub>1</sub>) excited state was optimized by time-dependent (TD) -DFT, employing the unrestricted UB3LYP method and the 6–31 + G(2d,p) basis set. All optimizations were carried out using a polarized continuum model to account for the solvent effects. Single-point calculations were carried out using the CAM-B3LYP functional and 6–31 + G(2d,p) basis set. CAM-B3LYP is especially suited for the TD-DFT calculations, in which CT states have to be considered.<sup>[23]</sup> Redox potentials of PPO were obtained from DFT calculations using a modification of a previously reported methodology for the estimation of SET potentials.<sup>[24]</sup> This approach has been previously applied.<sup>[16]</sup> The geometries of the radical cation and neutral species were optimized at the aug-cc-pVTZ basis set at UB3LYP level using the PCM model to account for the solvation.

### Acknowledgements

Financial support by the Marie Curie program of the E.U. (PIEFGA-2013-625064, R.P.R.) and the DFG Graduate School Photocatalysis (M.M.) is gratefully acknowledged. We thank Fabian Brandl (Univ. Regensburg) for time-resolved fluorescence measurements, Dr. Diego Sampedro (Univ. de la Rioja) for the theo-

retical calculation of the reduction potential of PPO, and Regina Hoheisel for CV measurements.

**Keywords:** aryl halides · defunctionalization · organocatalysis · photocatalysis · triplet states · two-photon process

- [1] a) A. G. Griesbeck, M. Oelgemöller, F. Ghetti, *CRC Handbook of Organic Photochemistry and Photobiology*, 3rd ed., CRC Press, Boca Raton, 2012; b) V. Balzani, P. Ceroni, A. Juris, *Photochemistry and Photophysics: Concepts, Research, Applications*, Wiley-VCH, Weinheim, 2014.
- [2] a) D. M. Schultz, T. P. Yoon, *Science* 2014, 343, 1239176; b) D. Ravelli, S. Protti, M. Fagnoni, A. Albini, *Curr. Org. Chem.* 2013, 17, 2366; c) C. K. Prier, D. A. Rankic, D. W. C. MacMillan, *Chem. Rev.* 2013, 113, 5322; d) M. Reckenthäler, A. G. Griesbeck, *Adv. Synth. Catal.* 2013, 355, 2727; e) J. W. Tucker, C. R. J. Stephenson, *J. Org. Chem.* 2012, 77, 1617; f) J. Xuan, W.-J. Xiao, *Angew. Chem. Int. Ed.* 2012, 51, 6828; *Angew. Chem.* 2012, 124, 6934; g) F. Teplý, *Collect. Czech. Chem. Commun.* 2011, 76, 859.
- [3] Other mechanisms operate in such bond activations. For some recent examples, see: a) Two-photon process: I. Ghosh, T. Ghosh, J. I. Bardagi, B. König, *Science* 2014, 346, 725; b) by UV irradiation: E. Abitelli, S. Protti, M. Fagnoni, A. Albini, *J. Org. Chem.* 2012, 77, 3501; c) via N-oxidation: L. Shi, W. Xia, *Chem. Soc. Rev.* 2012, 41, 7687; d) via H atom transfer: S. Protti, M. Fagnoni, D. Ravelli, *ChemCatChem* 2015, 7, 1516; e) via amine oxidation: C. K. Prier, D. W. C. MacMillan, *Chem. Sci.* 2014, 5, 4173; f) metal co-catalysis: D. C. Fabry, J. Zoller, S. Raja, M. Rueping, *Angew. Chem. Int. Ed.* 2014, 53, 10228; *Angew. Chem.* 2014, 126, 10392; g) H. Kim, C. Lee, *Angew. Chem. Int. Ed.* 2012, 51, 12303; *Angew. Chem.* 2012, 124, 12469.
- [4] Selected examples: a) D. Kalyani, K. B. McMurtrey, S. R. Neufeldt, M. S. Sanford, *J. Am. Chem. Soc.* 2011, 133, 18566; b) J. D. Nguyen, E. M. D'Amato, J. M. R. Narayanan, C. R. J. Stephenson, *Nat. Chem.* 2012, 4, 854; c) D. P. Hari, P. Schroll, B. König, *J. Am. Chem. Soc.* 2012, 134, 2958. Recent examples from our group: d) M. Majek, A. Jacobi von Wangelin, *Chem. Commun.* 2013, 49, 5507; e) M. Majek, F. Filace, A. Jacobi von Wangelin, *Beilstein J. Org. Chem.* 2014, 10, 981; f) M. Majek, A. Jacobi von Wangelin, *Angew. Chem. Int. Ed.* 2015, 54, 2270; *Angew. Chem.* 2015, 127, 2298.
- [5] Reduction potentials of aryl halides: C. P. Andrieux, C. Blocman, J.-M. Dumas-Bouchiat, J.-M. Saveant, *J. Am. Chem. Soc.* 1979, 101, 3431.
- [6] For a compilation of dyes and their redox potentials, see: <http://brsmblog.com/diroccos-electrochemical-series-photocatalysts/> (accessed July 12<sup>th</sup>, 2015) and refs. [2–4].
- [7] a) T. F. Schulze, T. W. Schmidt, *Energy Environ. Sci.* 2015, 8, 103; b) G. Chen, H. Qiu, P. N. Prasad, X. Chen, *Chem. Rev.* 2014, 114, 5161; c) F. Auzel, *Chem. Rev.* 2004, 104, 139; d) F. N. Castellano, T. J. Schmidt, *J. Phys. Chem. Lett.* 2014, 5, 4062.
- [8] a) Recent review article: T. N. Singh-Rachford, F. N. Castellano, *Coord. Chem. Rev.* 2010, 254, 2560; b) C. A. Parker, C. G. Hatchard, *Proc. R. Soc. London Ser. A* 1962, 269, 574; c) C. A. Parker, C. G. Hatchard, *Proc. Chem. Soc. London* 1962, 386; d) C. A. Parker, *Proc. R. Soc. London Ser. A* 1963, 276, 125. Selected recent examples: e) N. Adarsh, R. R. Avirah, D. Ramaiyah, *Org. Lett.* 2010, 12, 5720; f) T. Gallavardin, C. Armagnat, O. Maury, P. L. Baldeck, M. Lindgren, C. Monnerau, C. Andraud, *Chem. Commun.* 2012, 48, 1689; g) W. Wu, H. Guo, W. Wu, S. Ji, J. J. Zhao, *J. Org. Chem.* 2011, 76, 7056; h) T. Yogo, Y. Urano, Y. Ishitsuka, F. Maniwa, T. Nagano, *J. Am. Chem. Soc.* 2005, 127, 12162; i) S. Guo, W. Wu, H. Guo, J. Zhao, *J. Org. Chem.* 2012, 77, 3933; j) D. V. Kozlov, F. N. Castellano, *Chem. Commun.* 2004, 2860; k) R. R. Islangulov, D. V. Kozlov, F. N. Castellano, *Chem. Commun.* 2005, 3776; l) T. N. Singh-Rachford, R. R. Islangulov, F. N. Castellano, *J. Phys. Chem. A* 2008, 112, 3906; m) P. Du, R. Eisenberg, *Chem. Sci.* 2010, 1, 502; n) W. Zhao, F. N. Castellano, *J. Phys. Chem. A* 2006, 110, 11440; o) C. E. McCusker, F. N. Castellano, *Chem. Commun.* 2013, 49, 3537; p) J. Zhao, S. Ji, H. Guo, *RSC Adv.* 2011, 1, 937; q) R. R. Islangulov, F. N. Castellano, *Angew. Chem. Int. Ed.* 2006, 45, 5957; *Angew. Chem.* 2006, 118, 6103; r) R. S. Khnayzer, J. Blumhoff, J. A. Harrington, A. Haefele, F. Deng, F. N. Castellano, *Chem. Commun.* 2012, 48, 209; s) K. Börjesson, D. Dzebo, B. Albinsson, K. Moth-Poulsen, *J. Mater. Chem. A* 2013, 1, 8521.

- [9] a) C. Costentin, M. Robert, J.-M. Savéant, *J. Am. Chem. Soc.* **2004**, *126*, 16051; b) R. A. Rossi, *Acc. Chem. Res.* **1982**, *15*, 164; c) J. I. Bardagi, V. A. Vaillard, R. A. Rossi in *Encyclopedia of Radicals in Chemistry, Biology and Materials* (Eds.: C. Chatgililoglu, A. Studer), Wiley, Hoboken, **2012**, p.333.
- [10] T. N. Singh-Rachford, F. N. Castellano, *J. Phys. Chem. A* **2009**, *113*, 5912.
- [11] For laser equipment and spectroscopic set-up, see: R.-J. Kutta, T. Langenbacher, U. Kensy, B. Dick, *Appl. Phys. B* **2013**, *111*, 203.
- [12] A. D. McNaught, A. Wilkinson, *IUPAC Compendium of Chemical Terminology*, RSC, Cambridge, **1997**. <http://old.iupac.org/goldbook/D01579.pdf> (accessed June 5<sup>th</sup>, **2015**).
- [13] J. R. Lakowicz, *Principles of Fluorescence Spectroscopy*, 2nd ed., Kluwer/Plenum, New York, **1999**.
- [14] N. Nijegorodov, R. Mabbs, *Spectrochim. Acta Part A* **2000**, *56*, 2157.
- [15] A. Weller, *Z. Phys. Chem. (Muenchen Ger.)* **1982**, *133*, 93.
- [16] M. Majek, F. Filace, A. Jacobi von Wangelin, *Chem. Eur. J.* **2015**, *21*, 4518.
- [17] a) R. A. Marcus, *Pure Appl. Chem.* **1997**, *69*, 13; b) The nuclear reorganization energy  $\lambda$  was calculated by a method proposed by Nelsen and co-workers: S. F. Nelsen, M. N. Weaver, Y. Luo, J. R. Pladziewicz, L. K. Ausman, T. L. Jentzsch, J. J. O'Knek, *J. Phys. Chem. A* **2006**, *110*, 11665.
- [18] The quantum yield of the upconversion process under our conditions in DMF is 0.0012. See ref. [10] for a related system in benzene.
- [19] S. Ionescu, D. Popovici, A. T. Balaban, M. Hillebrand, *Spectrochim. Acta Part A* **2005**, *62*, 252.
- [20] S. Aich, C. Raha, S. Basu, *J. Chem. Soc. Faraday Trans.* **1997**, 2991.
- [21] V. V. Pavlishchuk, A. W. Addison, *Inorg. Chim. Acta* **2000**, *298*, 97.
- [22] Gaussian 09, Revision D.01, M. J. Frisch, G. W. Trucks, H. B. Schlegel, G. E. Scuseria, M. A. Robb, J. R. Cheeseman, G. Scalmani, V. Barone, B. Menucci, G. A. Petersson, H. Nakatsuji, M. Caricato, X. Li, H. P. Hratchian, A. F. Izmaylov, J. Bloino, G. Zheng, J. L. Sonnenberg, M. Hada, M. Ehara, K. Toyota, R. Fukuda, J. Hasegawa, M. Ishida, T. Nakajima, Y. Honda, O. Kitao, H. Nakai, T. Vreven, J. A. Montgomery, Jr., J. E. Peralta, F. Ogliaro, M. Bearpark, J. J. Heyd, E. Brothers, K. N. Kudin, V. N. Staroverov, R. Kobayashi, J. Normand, K. Raghavachari, A. Rendell, J. C. Burant, S. S. Iyengar, J. Tomasi, M. Cossi, N. Rega, J. M. Millam, M. Klene, J. E. Knox, J. B. Cross, V. Bakken, C. Adamo, J. Jaramillo, R. Gomperts, R. E. Stratmann, O. Yazyev, A. J. Austin, R. Cammi, C. Pomelli, J. W. Ochterski, R. L. Martin, K. Morokuma, V. G. Zakrzewski, G. A. Voth, P. Salvador, J. J. Dannenberg, S. Dapprich, A. D. Daniels, Ö. Farkas, J. B. Foresman, J. V. Ortiz, J. Cioslowski, and D. J. Fox, Gaussian, Inc., Wallingford CT, **2009**.
- [23] T. Yanai, D. P. Tew, N. C. Handy, *Chem. Phys. Lett.* **2004**, *393*, 51.
- [24] M.-H. Baik, R. A. Friesner, *J. Phys. Chem. A* **2002**, *106*, 7407.

---

Received: July 9, 2015

Published online on September 14, 2015